Figure 4 shows the scale effect on the wall pressure and temperature profiles. It can be seen that the wall pressure is unaffected by the scale change while the surface temperature presents some differences, especially in the divergent section with the scaled nozzle experiencing a lower wall temperature. The knee visible in the wall temperature distribution is due to the change of curvature between the throat and the conical divergent section of the nozzle and is made more evident by the scaled nozzle. Considering the following heterogeneous oxidizing reactions:

$$C_{(s)} + H_2O \rightleftharpoons CO + H_2\,;$$
$$C_{(s)} + CO_2 \rightleftharpoons 2CO\,,$$

it can be seen that a single mole of solid carbon $C_{(s)}$ can be consumed either with a single mole of H_2O or CO_2. Hence, the erosion rate contribution due to each oxidizing species can be obtained by mass conservation equation considering that each oxidizing species diffusing to the nozzle wall is completely consumed at the surface (diffusion-limited regime). The more oxidizing species are diffused to the surface, the more the nozzle surface is consumed.

Figure 5 shows the wall diffusive mass fluxes of the two oxidizing species, H_2O and CO_2. It can be clearly seen that the mass flow rate of the oxidizing species is higher for the scaled nozzle due to the scale effect on the boundary-layer structure.

Higher diffusion of oxidizing species leads to higher erosion rate as confirmed by Fig. 6*a* where the erosion rate at the throat is increased by 20% in the scaled nozzle. Note that this increase is even more severe in terms of throat area increase and, hence, performance loss, due to the lower throat radius. Figure 6*b* shows the convective heat flux distributions for the two cases with the scaled nozzle showing a higher heat flux. The nozzle scaling has a clear effect on the boundary layer structure leading to an increase of the diffusive mass and energy transfer and, hence, to a higher heat flux and erosion rate. A higher convective heat flux produces an increase of surface temperature while a higher erosion rate produces a reduction of surface temperature because of the heat absorption of the ablation process. However, due to the nonlinear nature of the surface mass and energy balance coupling (1) and (2), the surface temperature is reduced in the scaled geometry as shown in Fig. 4*b*.

The effect of the boundary layer thickness on the erosion process is now analyzed. As Fig. 6 clearly shows, there is a clear correlation between the heat flux distribution and the erosion rate distribution. Because the convective heat transfer depends on boundary layer evolution, it is important to analyze the boundary layer growth on rocket nozzle walls. In rapidly accelerating flows, like those inside a rocket nozzle, the boundary layer thickness may decrease in the flow direction, reaching a minimum at the throat section.

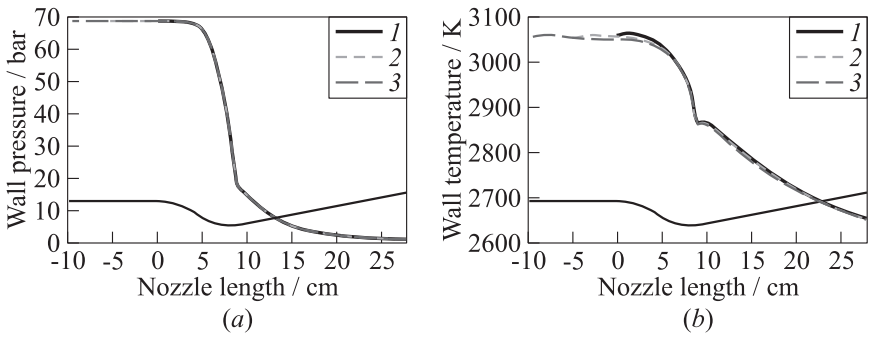

Figure 7 Boundary layer thickness effect on wall pressure (a) and temperature (b): *1* — $x_c = 0$; *2* — $0.5l_c$; and *3* — $x_c = l_c$. Thin curve — nozzle contour

This effect has been first demonstrated by the approximate calculation of Bartz [15] who made the following conclusions:

(i) the value of the boundary layer thickness tends to be a minimum near the throat, causing a maximum heat transfer rate in this section; and

(ii) the boundary layer thickness is not strongly dependent on the boundary layer thickness at entrance to the nozzle.

The first conclusion is a well established knowledge and Fig. 6 shows that the erosion rate follows the same trend as the convective heat flux with a maximum a bit ahead of the throat. To analyze the effect of the boundary layer thickness at the nozzle inlet, a constant area duct is added upstream of the inlet section (one equal to one half of the convergent length and one equal to one convergent length) to produce a larger boundary layer thickness at the inlet section. The obtained results show almost no differences in the core-flow region as for the scale effect analysis.

Figure 7 shows the effect of entrance boundary layer thickness on the wall pressure and temperature profiles. In this case, neither the surface pressure nor the surface temperature are affected by the boundary layer thickness at the nozzle entrance.

Figures 8 and 9 show the effect of duct length on the diffusive mass flux of oxidizing species, erosion rate, and convective heat flux distributions. Adding a constant area duct ahead of the nozzle inlet section generates a larger boundary layer thickness at the nozzle entrance, hence reducing the gradients and consequently the diffusive mass and energy fluxes. This effect is more evident in the convergent section, is reduced after the throat, and finally almost vanishes at the nozzle exit. Even if it can be concluded that the boundary layer thickness is

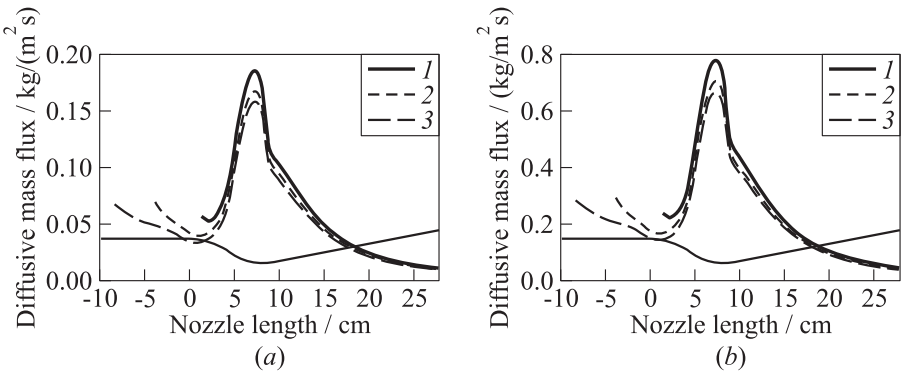

Figure 8 Boundary layer thickness effect (*1* — $x_c = 0$; *2* — $0.5l_c$; and *3* — $x_c = l_c$) on oxidizing species diffusion: CO_2 (*a*) and H_2O (*b*) wall diffusive mass flux. Thin curve — nozzle contour

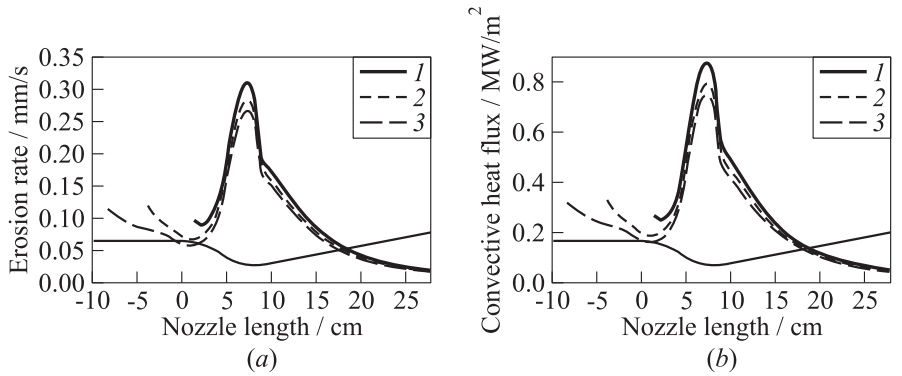

Figure 9 Boundary layer thickness effect on erosion rate (*a*) and wall heat flux (*b*): *1* — $x_c = 0$; *2* — $0.5l_c$; and *3* — $x_c = l_c$. Thin curve — nozzle contour

not strongly dependent on its thickness at entrance, the latter affects both heat flux and erosion rate at the throat section.

Figure 10 shows the combined effect of the added duct length and scale reduction on the throat erosion rate. With a duct length of one half of the convergent length, the erosion rate of the reference nozzle is reduced by 9%. This reduction is not negligible, especially if the uncertainty on the boundary layer thickness at entrance is high. However, a 14 percent reduction is obtained for a duct length equal to one convergent length, showing that the erosion rate decreases less than linearly with the added duct length exhibiting an asymptotic

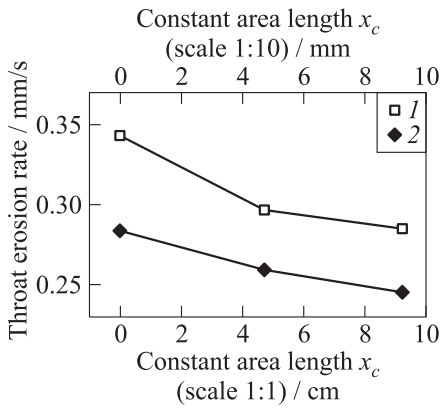

Figure 10 Scale and boundary layer thickness effect on throat erosion rate: *1* — scale 1:10; and *2* — scale 1:1

behavior. The scaled nozzle shows a similar trend with respect to the added length, with a more pronounced nonlinear behavior.

5 CONCLUDING REMARKS

A general model based on a full Navier–Stokes approach is adopted to examine both the scale and the inlet boundary layer thickness effect on the thermochemical ablation of C/C heat protection materials in SRM environments. This problem is of critical importance to predict nozzle erosion rate and, hence, motor performance.

The model includes all the relevant physics of the hot-gas flow, the ablation process, and the internal heat conduction into the material. The two regions, gas and solid, are coupled at the surface by appropriate energy and mass balances allowing the surface conditions to be solved as part of the overall solution. The surface thermochemistry model is based on heterogeneous chemical equilibrium and can account for both surface oxidation and sublimation. The results show that the nozzle scaling has a direct effect on the boundary layer structure leading to an increase of the diffusive mass and energy transfer and, hence, to a higher heat flux and erosion rate. From a performance perspective, this behavior is made even more severe by the reduced throat radius, which generates a higher area increase due to the reduced initial area. The results also show that the erosion rate at the throat section is sensitive to the boundary layer thickness at the nozzle entrance while its influence tend to vanish in the divergent section. This effect, which is basically due to the different boundary layer thickness in

the throat section and, hence, to the different heat and mass fluxes experienced, is made more evident by the reduction of the nozzle overall dimensions and, thus, could motivate the need for a better modeling of the boundary layer at the nozzle entrance.

ACKNOWLEDGMENTS

Authors acknowledge the contribution of A. Turchi for executing some of the presented computations during his graduation thesis.

REFERENCES

1. Delaney, L. J., L. C. Eagleton, and W. H. Jones. 1964. A semiquantitative prediction of the erosion of graphite nozzle inserts. *AIAA J.* 2(8).
2. McDonald, A. J., and P. O. Hedman. 1965. Erosion of graphite in solid-propellant combustion gases and effects on heat transfer. *AIAA J.* 3(7).
3. Klager, K. 1977. The interaction of the efflux of solid propellants with nozzle materials.*Propellants Explosives* 2(3):55–63.
4. Kuo, K. K., and S. T. Keswani. 1985. A comprehensive theoretical model for carbon–carbon composite recession. *Combust. Sci. Technol.* 42(3–4):145–64.
5. Keswani, S. T., and K. K. Kuo. 1986. Validation of an aerothermochemical model for graphite nozzle recession and heat-transfer processes. *Combust. Sci. Technol.* 47(3–4):177–92.
6. Borie, V., J. Brulard, and G. Lengelle. 1989. Aerothermochemical analysis of carbon–carbon nozzle regression in solid-propellant rocket motors. *J. Propul. Power* 5(6):665–73.
7. Geisler, R. L. 1981. The prediction of graphite rocket nozzle recession rates. *1981 JANNAF Propulsion Meeting Proceedings*. New Orleans, LA. CP/A Publication 342. 5:173–96.
8. Thakre, P., and V. Yang. 2008. Chemical erosion of carbon–carbon/graphite nozzles in solid-propellant rocket motors. *J. Propul. Power* 24(4):822–33.
9. Bianchi, D., F. Nasuti, and E. Martelli. 2009. Coupled analysis of flow and surface ablation in carbon–carbon rocket nozzles. *J. Spacecraft Rockets* 46(3).
10. Nasuti, E., and M. Onofri. 1996. Analysis of unsteady supersonic viscous flows by a shock fitting technique. *AIAA J.* 34(7):1428–34.
11. Moretti, G. 1987. A technique for integrating two-dimensional Euler equations. *Computer Fluids* 15(1):59–75.

12. Gordon, S., and B. J. McBride. 1994. Computer program for calculation of complex chemical equilibrium compositins and applications. NASA AP 1311.
13. Spalart, P. R., and S. R. Allmaras. 1994. A one-equation turbulence model for aerodynamic flow. *La Recherche Aerospatiale* 1:5–21.
14. Geisler, R. L., and C. W. Beckman. 1998. The history of the BATES Motors at the air force rocket propulsion laboratories. AIAA Paper No. 98-3981.
15. Bartz, D. R. 1955. An approximate form of compressible turbulent boundary layer development in convergent-divergent nozzles. *Trans. ASME* 77.